JOURNAL OF CATALYSIS **172,** 453–462 (1997)
ARTICLE NO. CA971893

Investigations of the Dispersion of Pd in H-ZSM-5

Adam W. Aylor, Lisa J. Lobree, Jeffrey A. Reimer, and Alexis T. Bell[1]

Chemical Sciences Division, Lawrence Berkeley National Laboratory and Department of Chemical Engineering, University of California, Berkeley, California 94720-1462

Received June 5, 1997; revised September 3, 1997; accepted September 4, 1997

The state of Pd dispersion in Pd–H-ZSM-5 was investigated by means of infrared spectroscopy and temperature-programmed desorption spectroscopy, using CO and NO as probe molecules. Following oxidation in O_2 at 773 K of a freshly prepared, low-loaded sample (Pd/Al = 0.048), most of the Pd is found to be present as isolated cations, viz. Pd^{n+} ($n = 1$–3). CO reduction at 773 K leads to the formation of Pd particles that fill the local pore space of the zeolite and are inaccessible to CO. Following CO reduction, oxidation in O_2 for 2 or 8 h at 773 K only partially redisperses the Pd. During treatment of a reduced sample in 5000 ppm NO for 60 min at 673 K, N_2O and N_2 are produced in an amount sufficient to oxidize all the Pd to PdO. Characterization of the state of Pd dispersion after NO pretreatment shows that all of the Pd has been redispersed as cations. Reoxidation of the reduced sample in NO is accompanied by a decrease in the infrared band due to Brønsted acid groups in an amount nearly equivalent to $2H^+$/Pd. Subsequent reduction of the sample regenerates the Brønsted acid band intensity. These observations suggest that isolated Pd cations may reside as $Z^-H^+(PdO)H^+Z^-$ in association with pairs of Al sites in the zeolite that are next-nearest neighbors. Following oxidation in O_2 at 773 K, a high-loaded sample of Pd–H-ZSM-5 (Pd/Al = 0.48) is found to have nearly the same concentration of highly dispersed Pd cations as the low-loaded sample, with the balance of the Pd in this case being present as small particles of PdO. Treatment of a reduced, high-loaded sample of Pd–H-ZSM-5 in NO at 773 K redisperses all of the Pd in structures that are proposed to be $Z^-H^+[(PdO)(NO)]H^+Z^-$ and $Z^-H^+[(PdO)(NO)]$. However, upon removal of the adsorbed NO by treatment in O_2 at 773 K, the $Z^-H^+[(PdO)(NO)]$ species revert to PdO, but the $Z^-H^+[(PdO)(NO)]H^+Z$ species remain stable as $Z^-H^+(PdO)H^+Z^-$. The present results suggest that maintenance of Pd in a high state of dispersion as isolated Pd^{n+} cations in the presence of O_2 at elevated temperatures requires pairs of next-nearest-neighbor Al sites in the zeolite.

INTRODUCTION

The performance of Pd-exchanged ZSM-5 for NO reduction by CH_4 in the presence of O_2 has been found to depend strongly on the initial form of the zeolite and the level of Pd exchange. Nishizaka and Misono (1) have shown that Pd exchanged into H-ZSM-5 is highly active but that Pd exchanged into Na-ZSM-5 is almost completely inactive. PdO clusters were observed by X-ray diffraction in the catalyst prepared from Na-ZSM-5, but not in the catalyst prepared from H-ZSM-5 (2). Based on these findings, it was concluded that acidity is essential for NO reduction by CH_4, and that one role of the acidity may be to stabilize Pd as isolated cations. In more recent studies, Resasco and co-workers (3) have found that the activity and selectivity of Pd–H-ZSM-5 for NO reduction by CH_4 in the presence of O_2 pass through maxima with increasing Pd loading, with the maxima occurring at about 0.3–0.4 wt% Pd. XANES and EXAFS observations of reduced Pd–H-ZSM-5 revealed the presence of small metallic particles of Pd for both low (0.3 wt% Pd) and high (1.0 wt% Pd) loaded samples (4). Following exposure of a reduced catalyst to the reaction mixture ($NO/CH_4/O_2$) isolated PdO species were found on the low-loaded Pd–H-ZSM-5, whereas PdO clusters were found on the high-loaded catalyst.

The preceding work suggests that Brønsted acid sites may play an important role in stabilizing Pd in a highly dispersed state and that this form of Pd is required to achieve high activity and selectivity for NO reduction by CH_4 in the presence of O_2. The goal of the present work was to determine the state of Pd in Pd–H-ZSM-5 and the effects of reduction and oxidation on the dispersion of Pd. Infrared spectroscopy of adsorbed CO and NO, together with temperature-programmed desorption of adsorbed CO, were used to probe the state of the dispersed Pd. Based upon prior studies conducted with Pd–Y (5, 6), oxidation in both O_2 and NO was investigated as a means for dispersing metallic Pd particles formed upon reduction of Pd cations associated with the ion-exchange sites in the zeolite. The effects of the Pd/Al ratio on the stability of Pd dispersion were also investigated as a part of this study.

EXPERIMENTAL

Na-ZSM-5 was obtained from UOP. This material was first converted to the NH_4^+ form. About 15 g of the zeolite was added to a 180 mL solution of 1.0 M ammonium

[1] Corresponding author.

0021-9517/97 $25.00

nitrate solution. This mixture was stirred at 298 K for 24 h, then filtered, and washed. This procedure was repeated two more times. Pd was exchanged into two batches of NH_4^+-ZSM-5. In the first [Pd–H-ZSM-5(L)], the NH_4^+-ZSM-5 was added to 125 mL of a 0.005 M $Pd(NO_3)_2 \cdot xH_2O$ solution at 333 K. In the second [Pd–H-ZSM-5(H)], NH_4^+-ZSM-5 was added to 1300 ml of a 0.005 M $Pd(NO_3)_2 \cdot xH_2O$ solution at 353 K. These solutions were stirred for 36 h (7) then filtered, washed, and dried overnight in a vacuum oven at 393 K. Based on elemental analysis of the exchanged samples, the Si/Al ratio was determined to be 16.1, and the Pd/Al ratios to be 0.048 (0.44 wt%) and 0.48 (4.14 wt%) for Pd–H-ZSM-5(L) and Pd–H-ZSM-5(H), respectively. The residual Na/Al < 0.01 for both samples.

For infrared spectroscopy, 20–50 mg of the palladium-exchanged zeolite was pressed into a self-supporting wafer and placed into an infrared cell similar to that described by Joly *et al*. (8). Spectra were recorded on a Digilab FTS-50 Fourier-transform infrared spectrometer at a resolution of 4 cm^{-1}. Typically, 64 scans were coadded to obtain a good signal-to-noise ratio. A reference spectrum of Pd–H-ZSM-5 in He, taken at the same temperature as the experimental spectrum, was subtracted from each spectrum. The temperature was increased at 1.0 k/min during the temperature-programmed infrared spectroscopy (TPD-IR) experiments.

Separate temperature-programmed desorption (TPD-MS) experiments were carried out with 0.1 g catalyst sieved to 35–60 mesh and placed in a quartz microreactor. Prior to each TPD-MS experiment, 4000 ppm CO was adsorbed on the catalyst at room temperature. The catalyst was purged with He for 1 h to remove weakly adsorbed species and then a temperature ramp of 8.0 K/min was initiated. CO was desorbed into He flowing at 100 cm^3/min; desorbing species were monitored via mass spectrometry (UTI 100 C).

For the present studies, 4.99% NO in He, 4.2% CO in He, and 10.1% O_2 in He were obtained from Matheson. UHP helium was obtained on-site. He, NO, and CO were passed through an oxysorb trap, an ascarite trap, and a molecular sieve trap, in that order, for additional purification. The O_2 was passed through an ascarite and a molecular sieve trap.

The freshly Pd-exchanged samples were heated at 773 K in He for 8 h to convert all residual NH_4^+ cations to H^+. Unless otherwise specified, prior to each experiment the catalyst was given one of the following pretreatments: (1) standard (S)—heat at 773 K in 10% O_2 for 2 h, heat at 773 K in He for 1 h, and cool to room temperature in He; (2) reductive (R)—heat at 773 K in 4.2% CO for 2 h, heat at 773 K in He for 1 h, and cool to the desired temperature in helium. Table 1 summarizes each of these catalyst pretreatment protocols.

For the redox cycles, a series of standard and reductive pretreatments were performed on Pd–H-ZSM-5(L) in the order S1, R1, S2, R2, S3, R3, S4. These are identified by pretreatment and cycle number. After each pretreatment, both CO TPD-IR and CO TPD-MS experiments were performed.

TABLE 1

Description of Catalyst Pretreatments

Symbol	Pretreatment	Step (1)	Step (2)	Step (3)	Step (4)
S	Standard	—	10% O_2 2 h	He 1 h	Cool in He
R	Reductive	—	4.2% CO 2 h	He 1 h	Cool in He
O/S	O_2/Standard	10% O_2 6 h	10% O_2 2 h	He 1 h	Cool in He
N/S	NO/Standard	0.5% NO 1 h	10% O_2 2 h	He 1 h	Cool in He

Note. Steps (1), (2), and (3) are conducted at 773 K.

RESULTS

Figure 1 shows the infrared spectrum taken at room temperature after a 20 min exposure of Pd–H-ZSM-5(L) to 4000 ppm CO following the standard pretreatment, S1. Sharp bands are observed at 2215, 2197, 2180, 2142, and 2128 cm^{-1}, with shoulders at 2185, 2170, and 2106 cm^{-1}. Smaller bands are observed at 1980 and 1895, and a broad set of features in the region of 1860–1770 cm^{-1}. The bands at 2215 and 2197 cm^{-1} are in close proximity to those observed by Sheu *et al*. (9) on Pd–Na–Y at 2218 and 2207 cm^{-1}. These features were assigned to CO adsorbed on Pd^{3+} in two different environments. However, when the catalyst is purged in He, the bands observed on Pd–H-ZSM-5(L) at 2215 and 2197 cm^{-1} decay together, suggesting that they may be due to $Pd^{3+}(CO)_2$. Bands at 2180 and 2142 cm^{-1} have been assigned to $Pd^{2+}(CO)$ in Pd–Na–Y (9) and, therefore, the bands at 2180 and 2142 cm^{-1} are assigned to $Pd^{2+}(CO)$ in two different environments. The feature at 2170 cm^{-1} can be assigned to CO adsorbed on Brønsted acid sites (10). A band assigned to $Pd^{+}(CO)$ has been observed at 2125 cm^{-1} on Pd/CeO_2 and 2130 cm^{-1} on Pd/Al_2O_3 (11). On this basis, we assign the band at 2128 cm^{-1} to $Pd^{+}(CO)$. Linear $Pd^0(CO)$ species yield bands near 2100 cm^{-1}, thus the band at 2106 cm^{-1} is assigned to $Pd^0(CO)$ (12). Bands below 2000 cm^{-1} are generally assigned to doubly and triply bridging CO on Pd particles. Therefore, the bands between 1900–2050 cm^{-1} are assigned to doubly bridging CO and bands below 1900 cm^{-1} are assigned to triply bridging CO associated with small metallic particles of Pd (13–16).

Also shown in Fig. 1 are a series of infrared spectra taken during temperature-programmed heating of the catalyst in He after it has been exposed to 4000 ppm of CO for 20 min at room temperature. Purging at room temperature causes little change in the spectrum. During the temperature ramp, the bands at 2215 and 2197 cm^{-1} disappear by 373 K, and the bands at 2185, 2180, 2142, and 2128 cm^{-1} disappear by 423 K, revealing a pair of bands at 2136 and 2118 cm^{-1}. These latter bands are assigned to $Pd^{2+}(CO)_2$ (17). The band at 2106 cm^{-1} first broadens, then decreases

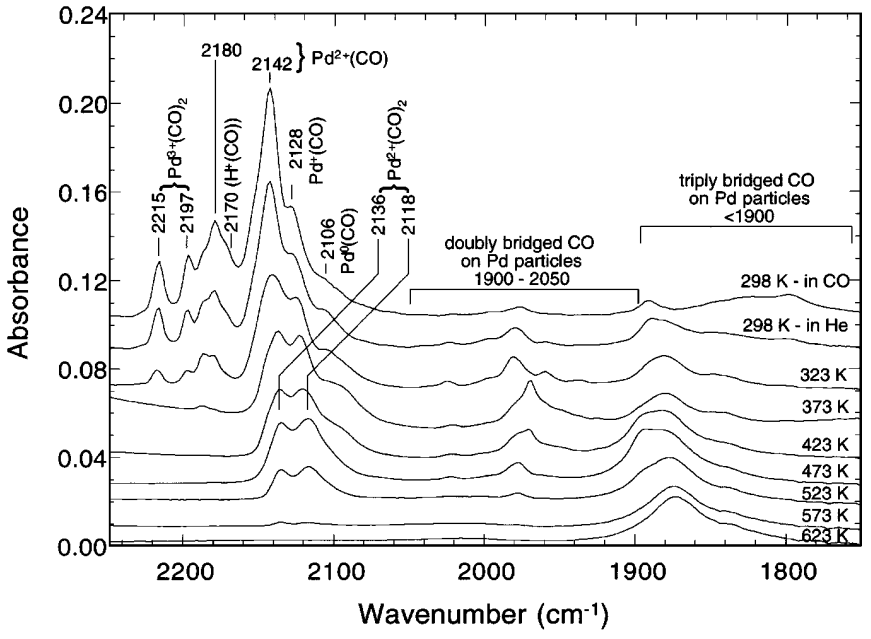

FIG. 1. Infrared spectra taken in 4000 ppm CO after 20 min of exposure of Pd–H-ZSM-5(L) at room temperature following pretreatment S1 and during temperature-programmed heating of the catalyst in He.

in intensity, and then completely disappears above 473 K. The bands between 2030 and 1920 cm^{-1} decrease monotonically with increasing temperature and disappear by 573 K. Careful inspection of the band at 1895 cm^{-1} shows an initial decrease in intensity with temperature up to 373 K. Above this temperature, the band at 1895 cm^{-1} increases in intensity, reaches a maximum intensity at 473 K, and then declines and completely disappears by 573 K. The bands at 1879 and 1843 cm^{-1} increase in intensity with temperature until 523 K and then decrease in intensity but are still visible up to 773 K.

Figure 2 shows the TPD spectrum for CO adsorbed on Pd–H-ZSM-5(L) given the initial standard pretreatment, S1. Prior to this experiment the catalyst is exposed to 4000 ppm of CO in He for 20 min at room temperature. CO desorbs in two major peaks at 355 and 600 K, whereas CO_2 exhibits three peak maxima at 375, 550, and 615 K. The peak at 615 K is followed by a long tail extending to 773 K. The total amount of CO that desorbs is 0.70 mol CO/mol Pd and the total amount of CO_2 desorbed is 0.14 mol CO/mol Pd. Thus the total amount of CO adsorbed is 0.84 mol CO/mol Pd.

During CO reduction (pretreatment R1) CO_2 is evolved from the sample. Infrared spectra taken during room temperature CO adsorption on the sample given pretreatment R1 and during the subsequent He purge are shown in Fig. 3. Prior to the He purge, features are observed in the range from 2000–2250 cm^{-1} and are attributed to gas phase CO. Superimposed on these bands is a sharp band at 2170 cm^{-1}; this band is again attributable to CO weakly adsorbed on the Brønsted acid sites. In the region below 2000 cm^{-1}, the only band present on the reduced catalyst is located at 1895 cm^{-1}. Following He purge the only feature remaining between 2000–2250 cm^{-1} is a small band at 2142 cm^{-1}. The band at 1895 cm^{-1} is unaffected by the He purge.

Figure 4 shows the hydroxyl stretching region for the catalyst after pretreatment R1 (a) and the difference between the spectra taken after pretreatments S1 and R1 (b). Three bands are observed in this range at 3740, 3660, and 3610 cm^{-1}. The band at 3740 cm^{-1} has been assigned to Si(OH) groups at crystal terminations and silanol pairs (18), whereas the feature at 3660 cm^{-1} has been assigned

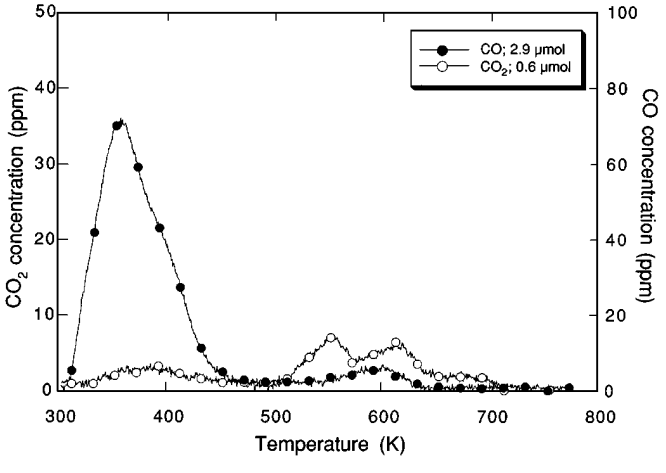

FIG. 2. Mass spectrometer signals for CO and CO_2 observed during temperature-programmed desorption following room temperature exposure of Pd–H-ZSM-5(L), given pretreatment S1, to 4000 ppm CO for 20 min. The total quantities of CO and CO desorbed are given in the inset.

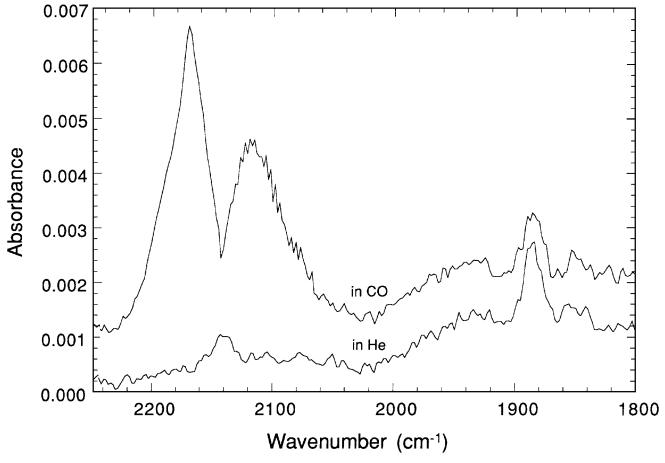

FIG. 3. Infrared spectra taken during room temperature exposure of Pd–H-ZSM-5(L), given pretreatment R1, to 4000 ppm CO in He, and during the subsequent He purge.

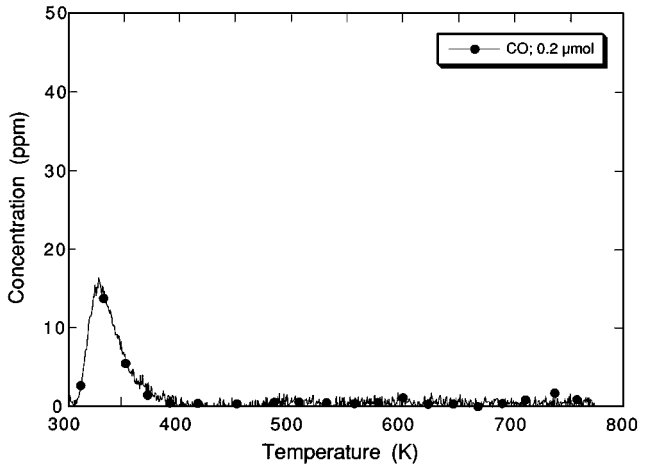

FIG. 5. Mass spectrometer signals for CO observed during temperature-programmed desorption following room-temperature exposure of Pd–H-ZSM-5(L), given pretreatment R1, to 4000 ppm CO for 20 min. The total amount of CO desorbed is shown in the inset.

to OH groups associated with extra-framework aluminum (19, 20). The band at 3610 cm^{-1} is due to the OH stretch of Brønsted acid groups (21). Subtraction of the spectrum taken after pretreatment R1 from the spectrum taken after S1 (b), results in the appearance of a negative band at 3610 cm^{-1}. This indicates that there is an increase in the quantity of Brønsted acid groups visible after CO reduction. The area of the feature at 3610 cm^{-1} in the difference spectrum is approximately 7.5% of the corresponding band area measured after pretreatment R1 (the maximum change in intensity of the 3610 cm^{-1} band was observed for the difference between treatments R4 and N/S; see below. A total change in the area of 8.2% was found which is the equivalent of 1.71 H^+/Pd). Hydroxyl groups other than the Brønsted acid groups are unaffected by the pretreatments. What this suggests is that the highly dispersed Pd may be secured as $Z^-H^+(PdO)H^+Z^-$, in which two Brønsted acid groups proximate to each other serve to stabilize a PdO molecule. It must be understood that the species $Z^-H^+(PdO)H^+Z^-$, while having the correct stoichiometry, may not represent the exact structure of the species.

CO TPD into He was performed following CO reduction, R1. The results are shown in Fig. 5. One peak for CO desorption is observed at 340 K. The integrated amount of CO observed on the reduced catalyst is only 7% of that observed on the catalyst given pretreatment S1. No CO_2 is observed in the TPD spectrum of the reduced catalyst. The CO TPD spectra taken after the pretreatments R2, R3, and R4, are nearly identical to those shown in Fig. 5.

Figure 6 shows a series of infrared spectra taken during CO TPD from Pd-ZSM-5(L) after pretreatment S2.

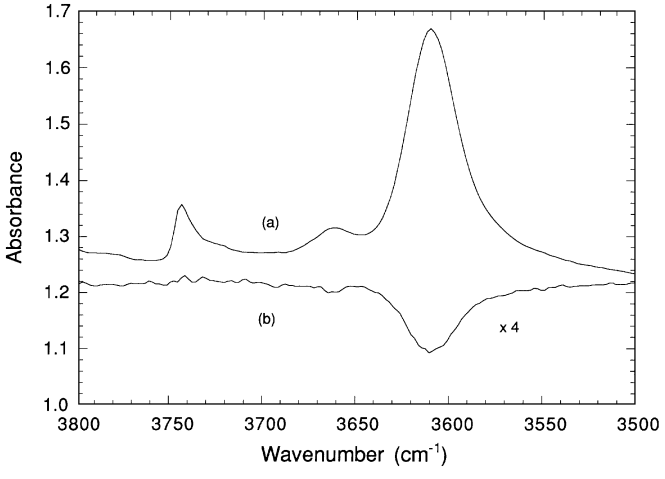

FIG. 4. Infrared spectra of the hydroxyl stretching region for Pd–H-ZSM-5(L) after pretreatment R1 (a) and the difference spectrum after the catalyst has been given pretreatments S1 and R1 (b).

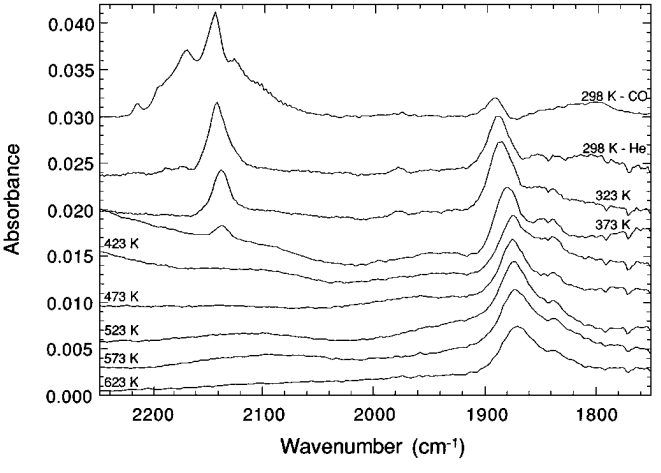

FIG. 6. Infrared spectra taken in CO at room temperature and during temperature-programmed desorption after 20 min exposure of Pd–H-ZSM-5(L), given pretreatment S2, to 4000 ppm CO in He.

The room-temperature spectrum is qualitatively similar to that obtained after pretreatment S1 but the intensity of the bands between 2050 and 2300 cm^{-1} is much lower, and the bands between 1920 and 2050 cm^{-1} are nearly absent. During the He purge all bands above 2000 cm^{-1} disappear with the exception of the band due to $Pd^{2+}(CO)$ at 2142 cm^{-1}. Ramping the temperature causes the band at 2142 cm^{-1} to disappear by 423 K. After this pretreatment, the band at 1895 cm^{-1} does not reappear during the temperature ramp. The bands at 1879 and 1843 cm^{-1} are once again present and persist to 773 K, although at a lower intensity. Infrared spectra taken during TPD following pretreatments, S3 and S4, are qualitatively similar to those shown in Fig. 6; however, the intensity of all bands decrease with each redox cycle.

TPD-MS spectra were taken after Pd–H-ZSM-5(L) had undergone pretreatments S2, S3, and S4. Since the appearance of the TPD spectra for CO and CO_2, following these pretreatments, are very similar (as an example of these spectra see Figs. 9A(b) and 9B(b)), only the integrated amounts of CO and CO_2 desorbed are shown in Fig. 7. It is evident that the CO adsorption capacity of the sample decreases monotonically with each standard pretreatment S1–S4. It is also apparent that after any R pretreatment the CO adsorption capacity is reduced to almost zero. The quantity of CO_2 desorbed after a standard pretreatment is nearly constant throughout the redox cycles and drops to zero following any of the R pretreatments.

From the results presented in Figs. 6 and 7 it is clear that a 2-h exposure of Pd–H-ZSM-5(L) to oxygen at 773 K (i.e., pretreatment S) is only partially effective in reversing the effects of CO reduction on the initial CO adsorption capacity observed by either infrared spectroscopy or TPD. To ascertain whether the initial CO adsorption capacity could be restored more completely, the sample was

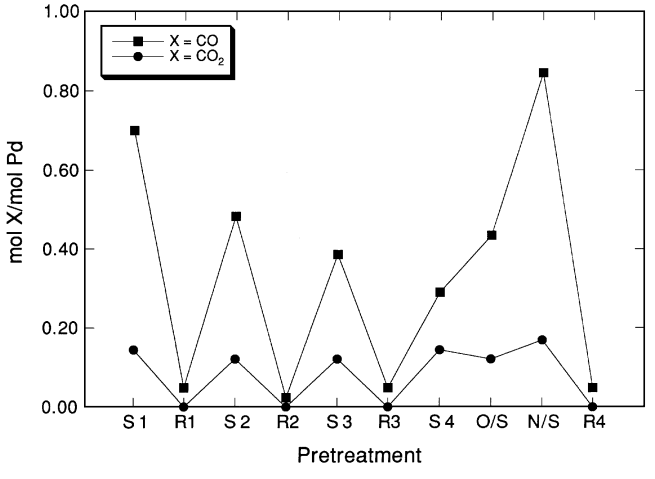

FIG. 7. Amounts of CO and CO_2 desorbed during temperature-programmed desorption in He following room-temperature exposure of Pd–H-ZSM-5(L) to 4000 ppm CO after various types of pretreatment.

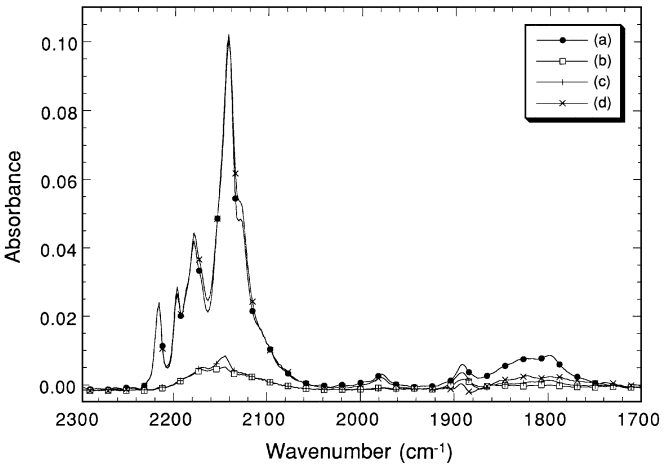

FIG. 8. Infrared spectra taken following room temperature exposure of Pd–H-ZSM-5(L) to 4000 ppm CO in He after pretreatments S1 (a), S4 (b), O/S (c), and N/S (d).

given either a 6-h exposure to 10% oxygen at 773 K followed by a standard pretreatment (O/S), or a 1-h exposure to 5000 ppm NO in He at 773 K followed by a standard pretreatment (N/S). The infrared spectrum of CO adsorbed at room temperature, and the CO TPD spectrum of CO after pretreatment S1 (a), pretreatment S4 (b), pretreatment O/S (c), and pretreatment N/S (d), are illustrated in Figs. 8 and 9, respectively. Figure 8 shows that the intensity of the bands for adsorbed CO decrease by a factor of about 10 when the spectrum taken after pretreatment S4 is compared with that taken after pretreatment S1. Pretreatment O/S, yields only a small increase in CO adsorption intensity. Pretreatment N/S, however, produces a room temperature CO adsorption spectrum nearly identical to that following pretreatment S1. The only difference is that the bands between 2020 and 2250 cm^{-1} are slightly more intense and the bands below 1920 cm^{-1} do not regain their initial intensity. It is also noted that after pretreatment N/S the series of infrared spectra recorded during TPD (not shown) look very similar to those shown in Fig. 1, with the exception of the bands at 1879 and 1843 cm^{-1}, due to CO adsorbed on Pd particles which are no longer present.

Figures 9A and B show the CO and CO_2 signals recorded during TPD following the pretreatments S1, S4, O/S, and N/S. Following pretreatment S4, the amount of CO desorbed is only about 40% of the amount of CO desorbed following pretreatment S1. In addition, the second CO desorption peak at 600 K is absent. Pretreatment O/S causes a 50% increase in the amount of CO desorbed relative to that desorbed after pretreatment S4. Pretreatment N/S raises the CO adsorption capacity to the point where it exceeds that observed after pretreatment S1 and causes the CO desorption spectrum to look qualitatively the same as that observed after pretreatment S1. Figure 9B shows the CO_2 desorption profiles. The total amount of CO_2 desorbing

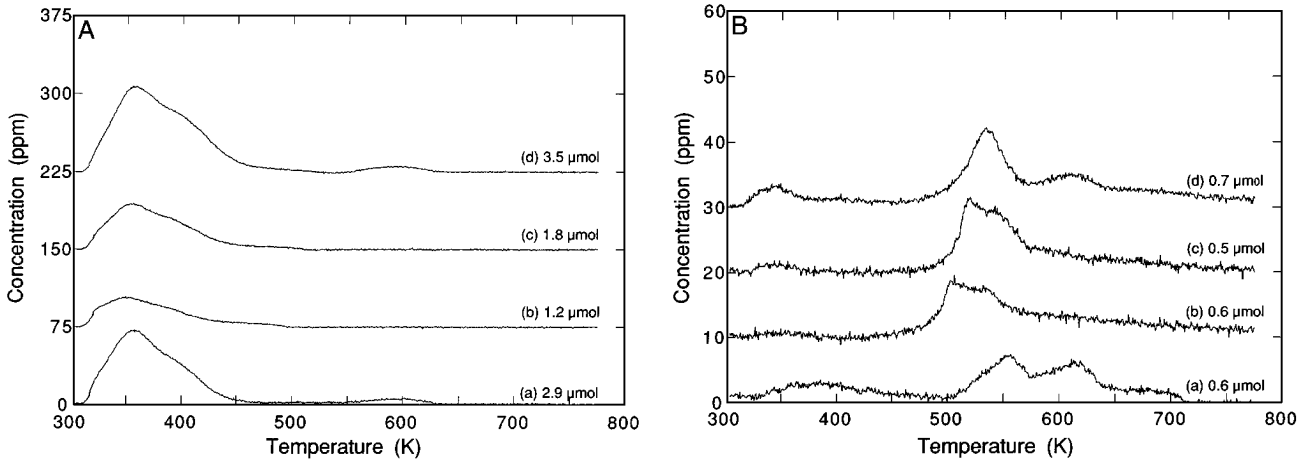

FIG. 9. A. Mass spectrometer signals for CO observed during temperature-programmed desorption in He following room-temperature exposure of Pd–H-ZSM-5(L) to 4000 ppm CO after pretreatment S1 (a), S4 (b), O/S (c), and N/S (d). The total amount of CO desorbed is shown on the right-hand side of each spectrum. B. Mass spectrometer signals for CO_2 observed during temperature-programmed desorption in He following room-temperature exposure of Pd–H-ZSM-5(L) to 4000 ppm CO after pretreatment S1 (a), S4 (b), O/S (c), and N/S (d). The total amount of CO_2 desorbed is shown on the right-hand side of each spectrum.

remains essentially unchanged by the nature of the pretreatment. However the appearance of the spectra does change. Pretreatment S4 causes the CO_2 desorption peak at 615 K to disappear, and the peak maximum at 550 K to drop in temperature and broaden. Following pretreatment O/S, the peak between 500 and 600 K shifts toward the higher temperature, opposite to what occurred following successive redox cycles (not shown). Pretreatment N/S causes this peak to narrow into a peak with a maximum at 530 K, and the peak at 615 K to reappear.

The total amounts of CO and CO_2 desorbed following pretreatments O/S, N/S, and R4 are shown in Fig. 7. CO desorption is raised by pretreatment O/S to about 0.42 mol CO/mol Pd, and by pretreatment N/S to about 0.85 mol CO/mol Pd. Subsequent CO reduction, pretreatment R4, again reduces CO desorption to near zero. CO_2 desorption is essentially unchanged by pretreatment O/S or N/S and drops to zero following pretreatment R4. Following pretreatment N/S, the ratio of CO_x/Pd is about 1.01. This, in conjunction with the observed elimination of infrared bands at 1879 and 1843 cm^{-1} (see above), indicates nearly atomic dispersion of Pd.

To follow the process of reoxidation and redispersion, a CO reduced catalyst was exposed to 5000 ppm NO at 673 K. Mass spectrometry signals for N_2O and N_2 were recorded as a function of time and are shown in Fig. 10. After 60 min, the amounts of N_2O and N_2 are 1.1 and 1.7 μmol, respectively. If it is assumed that these products result from the oxidation of Pd according to the reactions $NO + 0.5\ Pd \rightarrow 0.5\ N_2O + 0.5\ PdO$ and $NO + Pd \rightarrow 0.5\ N_2 + PdO$, then the total amount of Pd oxidized to PdO is 4.5 μmol, which agrees very closely with the amount of Pd in the sample, 4.1 μmol. From this it is concluded that CO reduction at 773 K converts virtually all of the initially dispersed Pd cations into metallic Pd particles, viz. $(Pd)_n$ and that NO oxidation at 773 K of the reduced sample fully redisperses the Pd as cations.

The redispersion of Pd by NO at 698 K was followed by infrared spectroscopy. As shown in Fig. 11A, a single band is observed at 1866 cm^{-1}, associated with NO adsorbed on molecularly dispersed PdO. With time the integrated intensity increases by nearly a factor of 5. Substitution of O_2 for NO at 698 K results in an almost complete disappearance of the band at 1866 cm^{-1} in 30 min, but upon reintroduction of NO (see Fig. 11B) the intensity of the band is restored immediately and then continues to increase. This experiment demonstrates that the Pd dispersion in Pd–H-ZSM-5(L), achieved by the reaction of $(Pd)_n$ with NO, is stable upon the removal of adsorbed NO.

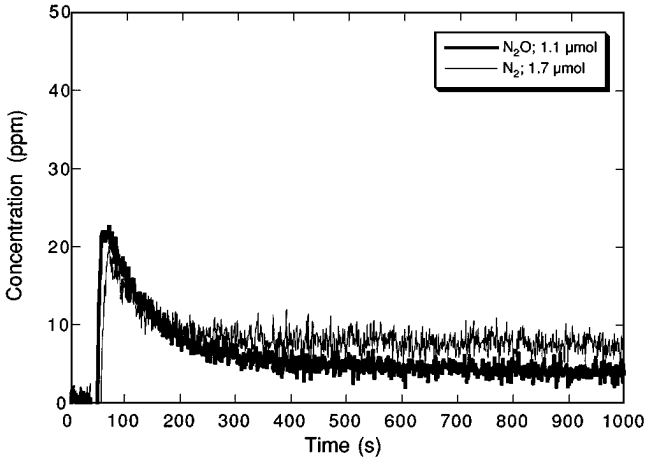

FIG. 10. Mass spectrometer signals for N_2O and N_2 observed during exposure of Pd–H-ZSM-5(L), given pretreatment R, to 5000 ppm NO at 673 K. The total amounts of N_2O and N_2 desorbed are shown in the inset.

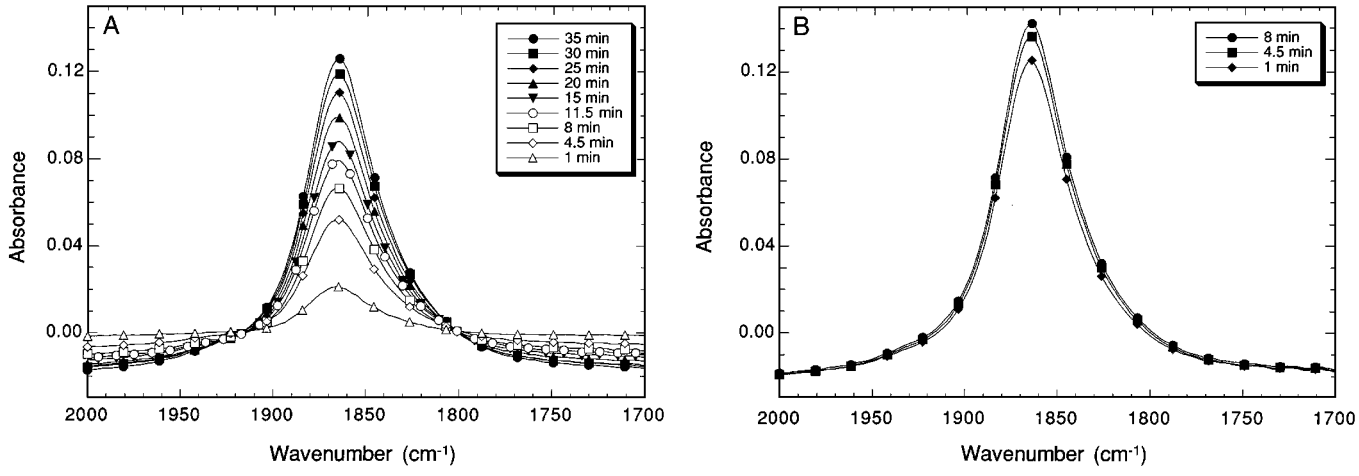

FIG. 11. A. Infrared spectra of Pd–H-ZSM-5(L) at 698 K in flowing NO (5000 ppm) following pretreatment R. B. Infrared spectra taken at 698 K after reintroduction of NO (5000 ppm) following 30 min of exposure to 10% O_2 at 698 K.

Pd–H-ZSM-5(H). To determine the effect of metal loading on Pd dispersion, Pd–H-ZSM-5(H) was investigated following pretreatments S1 and R1. Figure 12A compares the spectra for CO adsorbed on Pd–H-ZSM-5(H) and Pd–H-ZSM-5(L) after pretreatment S1. What is striking is that the intensities of the bands for adsorbed CO are very similar for samples of equivalent thickness, even though the high-loaded sample contains 10 times as much Pd. The only significant difference is that the bands at 2215 and 2197 cm^{-1} are more intense for the high-loaded sample, indicating a greater concentration of Pd^{3+} sites. The small band observed at 2360 cm^{-1} is due to weakly adsorbed CO_2. These results suggest that there are a limited number of sites capable of holding Pd in a highly dispersed state and that when the capacity of these sites is exceeded the remaining Pd forms into small clusters of PdO (i.e., $(PdO)_n$).

Following pretreatment R1, the spectrum for adsorbed CO on the high-loaded sample shows little evidence for CO adsorbed on Pd^{n+} ($n = 1$–3) or Pd^0 sites, much as in the case for the low-loaded sample (see Fig. 12B). The only difference is that for the high-loaded sample, a strong band appears at 2000 cm^{-1}. This band can be assigned to either linear or dibridge bonded CO on metallic Pd (13–16). There are also a series of overlapping bands in the region of 2000–1900 cm^{-1} characteristic of dibridge bonded CO on metallic Pd particles. Thus, as for the low-loaded sample, reduction in CO results in a complete loss of atomically dispersed Pd.

The adsorption of NO at room temperature on the high- and low-loaded samples of Pd–H-ZSM-5 following pretreatment S1 produces the spectra shown in Fig. 13A. Features are observed at 2130, 1880, and 1840 cm^{-1}. The band at 2130 cm^{-1} is assigned to NO_2 associated with Brønsted

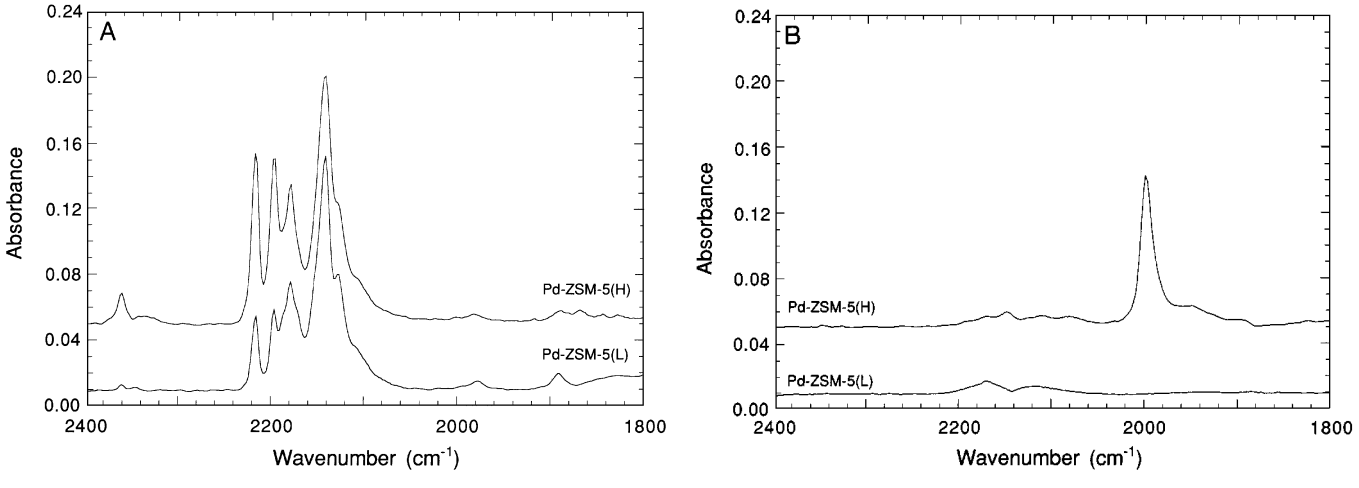

FIG. 12. A. Infrared spectra obtained during exposure of Pd-ZSM-5(H) and Pd-ZSM-5(L), given pretreatment S1, to 4200 ppm CO at room temperature. B. Infrared spectra obtained during exposure of Pd-ZSM-5(H) and Pd-ZSM-5(L), given pretreatment R1, to 4200 ppm CO at room temperature.

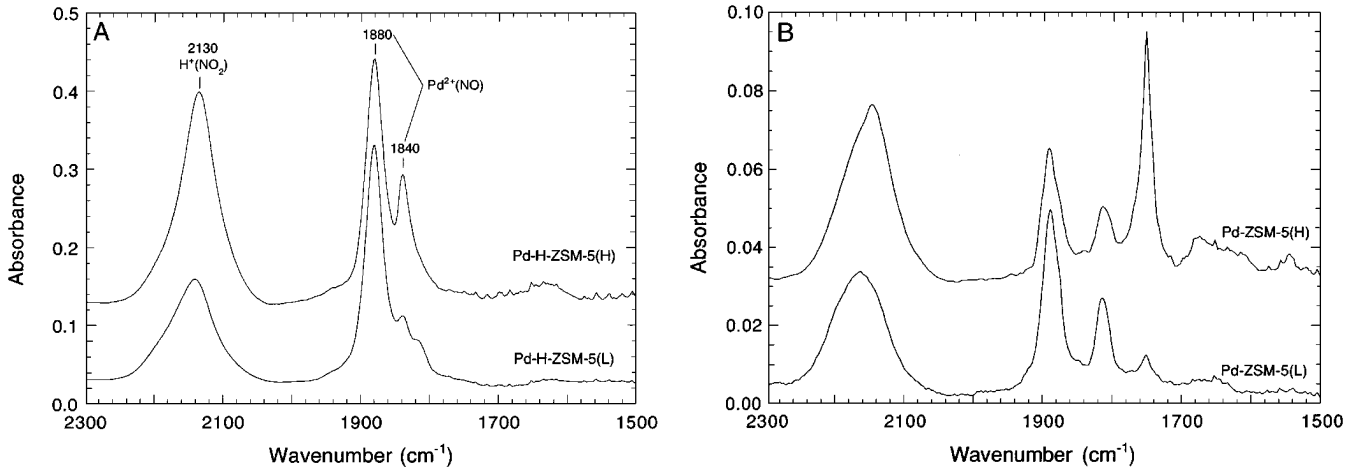

FIG. 13. A. Infrared spectra obtained during exposure of Pd-ZSM-5(H) and Pd-ZSM-5(L), given pretreatment S1, to 5000 ppm NO at room temperature. B. Infrared spectra obtained during exposure of Pd-ZSM-5(H) and Pd-ZSM-5(L), given pretreatment R1, to 5000 ppm NO at room temperature.

acid sites (22). The features at 1880 and 1840 cm^{-1} are very similar in position and relative intensity to the bands observed for NO adsorbed on Pd–Y and are assigned to NO adsorbed on Pd^{2+} cations in two different environments (23). Here too, the intensities of the bands associated with adsorbed NO on Pd cations are nearly identical in intensity for both samples.

Spectra of adsorbed NO taken following pretreatment R1 are presented in Fig. 13B. The intensities of all of the features are significantly weaker in this case than those in Fig. 13A. However, once again the intensities of the bands at 1892 and 1815 cm^{-1}, associated with NO adsorbed on residual Pd cations, are comparable for the high- and low-loaded samples. The new bands in both spectra appearing at 1753, 1630, and 1560 cm^{-1} are similar to those observed for NO adsorption on particles of Pd supported on silica (24). Not surprisingly, these bands are significantly more intense for the high- than for the low-loaded sample.

Temperature-programmed reaction of both samples of Pd–H-ZSM-5 was carried out in a stream containing 5000 ppm of NO in He. At 298 K, the infrared spectra are identical to those shown in Fig. 13A. With increasing temperatures all features disappeared except for a broad band at 1860 cm^{-1}. For the high-loaded sample the intensity of this feature grew with increasing temperature until it reached the level shown in Fig. 14 at 773 K. By contrast, for the low-loaded sample the intensity of the band at 1860 cm^{-1} decreases to the level seen in Fig. 14. The ratio of band intensities at 773 K for the two samples is approximately 10, in good accord with the ratio of the Pd content. In NO at 773 K, the intensity of the band at 3610 cm^{-1} for Brønsted acid hydroxyls dramatically decreases for the high-loaded sample (relative to a sample given pretreatment N/S), but it remains the same for the low-loaded sample. The decrease in intensity of the band for Brønsted acid groups on Pd–H-ZSM-5(H) is the equivalent of about 1 H^+/Pd. These observations suggest that temperature-programmed oxidation of the high-loaded sample by NO results in complete dispersion of the Pd initially present as $(PdO)_n$, and that at 773 K, the fractional coverage of isolated PdO species is the same on both samples. It also suggests that the (PdO)NO species are anchored at Brønsted acid sites. Purging the catalyst in He at 773 K for 1 h, following oxidation in NO, does not remove much of the adsorbed NO, reflecting a strong (PdO)–NO bond.

If, after oxidation in NO at 773 K, each of the Pd–H-ZSM-5 samples is heated in O_2 at 773 K, all residually adsorbed NO is removed. The catalyst is then purged in He at 773 K and cooled in He to room temperature (e.g., pretreatment N/S). Finally, after exposing the catalyst to

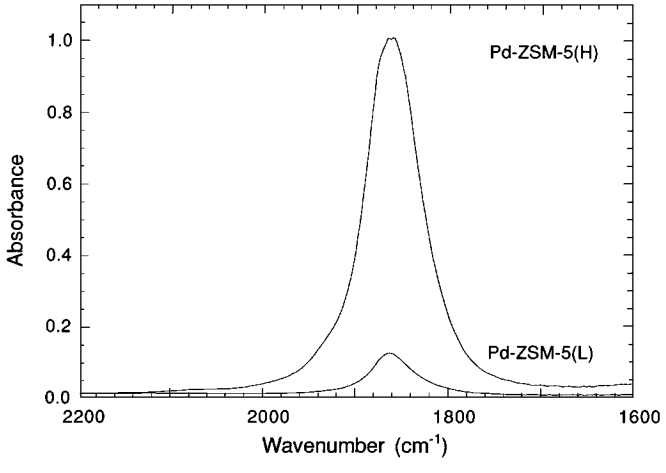

FIG. 14. Infrared spectra observed at 773 K following temperature-programmed reaction in a mixture containing 5000 ppm NO in He over Pd-ZSM-5(L) and Pd-ZSM-5(H). Each sample was exposed to the reaction mixture for 20 min at room temperature prior to the temperature ramp.

5000 ppm NO at room temperature, the spectra become identical to those seen in Fig. 13A. This suggests that the dispersion achieved by the temperature-programmed reaction in NO on the high-loaded sample is not stable once the adsorbed NO is removed. One way to interpret these observations is to suggest that the majority of the highly dispersed Pd in the high-loaded sample after the NO reaction at elevated temperatures is present as $Z^-H^+(PdO)NO$. Upon release of the adsorbed NO one can imagine that Z^-H^+PdO is formed and that PdO held in this manner is less stable to agglomeration into $(PdO)_n$ than PdO held as $Z^-H^+(PdO)H^+Z^-$.

DISCUSSION

The present study clearly demonstrates that the state of Pd in Pd–H-ZSM-5 is a strong function of both the manner in which the catalyst has been pretreated and the loading of Pd. TPD-MS experiments performed following room temperature adsorption of CO on a freshly prepared sample of Pd–H-ZSM-5(L) given pretreatment S1, show a CO_x/Pd ratio of about 0.84. This suggests that virtually all of the Pd is present as isolated species. The infrared spectra indicate that most of the Pd is present as Pd^{n+} ($n = 1$–3). Infrared spectra taken during CO adsorption on Pd–H-ZSM-5(H) given pretreatment S1 show nearly the same amount of Pd^{n+} present. This suggests that the remainder of the Pd in Pd–H-ZSM-5(H) is present as particles of PdO. Consistent with this idea, Raman spectra taken of oxidized Pd–H-ZSM-5(H) showed an intense band at 651 cm^{-1} representative of bulk PdO (25). This band is absent, however, in an oxidized sample of Pd–H-ZSM-5(L). The Pd cations may be associated with the zeolite either as charge compensating species, viz. $Z^-Pd^{n+}(OH^-)_{(n-1)}$, or as neutral PdO species attached to the zeolite via interactions with Brønsted acid sites, viz. $Z^-H^+(PdO)$ and $Z^-H^+(PdO)H^+Z^-$. The driving force for PdO to remain anchored at Brønsted acid sites is presumably the bonding between the acidic proton and the Pd in a manner similar to that proposed for small Pd clusters in Pd–Y (26, 27). Following CO reduction, pretreatment R1, the CO adsorption capacity of Pd–H-ZSM-5(L) is greatly reduced as judged both by infrared spectroscopy and TPD. There is, however, an increase in the intensity of the band at 3610 cm^{-1} associated with O–H stretches of Brønsted acid sites. Since CO reduction does not involve the addition of protons to the zeolite, it must be assumed that the protons were already present. The observed changes might be attributed to processes such as

1. $n\ Z^-Pd^{2+}(OH^-) + n\ CO \rightarrow n\ Z^-H^+ + Pd_n + n\ CO_2$
2. $n\ Z^-H^+(PdO) + n\ CO \rightarrow n\ Z^-H^+ + Pd_n + n\ CO_2$
3. $n\ Z^-H^+(PdO)H^+Z^- + n\ CO \rightarrow 2n\ Z^-H^+ + Pd_n + n\ CO_2$

In reactions 1–3, Pd_n represents small Pd clusters. The formation of such clusters is suggested by complete loss of CO bands characteristic of interaction with Pd^{n+} ($n = 1$–3) cations upon CO reduction and the observation that high temperature oxidation of reduced Pd–H-ZSM-5(L) by NO consumed the stoichiometric amount of oxygen required to oxidize all of the Pd^0 to PdO. Further evidence for the formation of Pd_n clusters is provided by the growth in intensity of the bands in the region below 2000 cm^{-1} during TPD of CO on Pd–H-ZSM-5(L) following pretreatment S1 (see Fig. 1), since these bands are attributed to triply bridging CO on metallic Pd particles. It is notable that these bands are not visible after the sample has received pretreatment R1. This suggests that high temperature reduction of the sample creates Pd particles that are large enough to completely fill the local pore space in the zeolite, thereby limiting access of CO. The observation that the increase in the intensity of the band at 3610 cm^{-1}, on Pd–H-ZSM-5(L) after pretreatment R1, corresponds to the appearance of nearly two Brønsted acid protons per Pd suggests that most of the initially exchanged Pd is present as $Z^-H^+(PdO)H^+Z^-$. Stabilization of PdO in this manner implies the presence of pairs of next-nearest-neighbor Al sites in the zeolite. While random distribution of Al in ZSM-5 allows for only 1% of all the Al to occur in such sites, chemiluminescence measurements on Cu-ZSM-5 (Si/Al = 22.6) suggest that the percentage may be as high as 30% (28). For the present sample of ZSM-5, we would infer that the proportion of Al pairs is of the order 10% of the Al, since above a Pd/Al ratio of about 0.05, Pd cannot be maintained in a high state of dispersion.

Oxidation of previously reduced Pd–H-ZSM-5 during pretreatment S_n ($n > 1$) or O/S is only partially successful in redispersing the Pd that has formed into Pd_n clusters. Figures 7 and 8 show that only a fraction of the original CO adsorption capacity is recovered by such pretreatments. The elementary processes envisioned to occur during high temperature oxidation in O_2 are

4. $Pd_n + n/2\ O_2 = (PdO)_n$
5. $(PdO)_n = (PdO)_{(n-1)} + PdO$
6. $2\ Z^-H^+ + PdO \rightarrow Z^-H^+(PdO)H^+Z^-$.

The redispersion of Pd upon oxidation in NO is far more successful than when oxidation is carried out in O_2, as is clearly evident from Figs. 7–9. During oxidation in NO both N_2O and N_2 are presumably formed via the processes:

7. $Pd_n + 2n\ NO \rightarrow (PdO)_n + n\ N_2O$
8. $Pd_n + n\ NO \rightarrow (PdO)_n + n/2\ N_2$.

As noted in connection with Fig. 10, the total amount of nitrogen-containing products produced upon oxidation of the sample following CO reduction is consistent with the complete oxidation of the Pd to PdO. The mechanism by which NO promotes the redispersion of Pd is not well defined. One may imagine, for example, that NO reacts with the PdO formed in reaction 5, yielding volatile (PdO)NO

species which then diffuse through the zeolite and are stabilized by reaction with Brønsted acid sites. These two processes can be written as

9. $(PdO)_n + NO = (PdO)_{(n-1)} + (PdO)NO$
10. $(PdO)NO + 2\ Z^-H^+ \rightarrow Z^-H^+[(PdO)NO]H^+Z^-$.

The strength of the PdO–(NO) bond, discussed in conjunction with Fig. 14, drives the redispersion of $(PdO)_n$ to a greater extent then the processes suggested by reactions 5 and 6. Desorption of NO from the product of reaction 10 then yields $Z^-H^+(PdO)H^+Z^-$. Consistent with this picture of the redispersion process, the intensity of the band at 3610 cm^{-1} for Brønsted acid bridging hydroxyls decreases by an amount corresponding to roughly two hydroxyl groups per Pd. The effectiveness of reaction 9 versus reaction 5 in dispersing PdO is supported by recent quantum density functional theory calculations which show that the process $PdO + NO \rightarrow PdO(NO)$ is significantly exothermic (29).

When the Pd loading is increased from Pd/Al = 0.048 to Pd/Al = 0.48, pretreatment N/S again appears to achieve complete dispersion of the Pd, but in this case the dispersion of the majority of the Pd is not stable. The portion held as $Z^-H^+(PdO)H^+Z^-$ remains well dispersed but the portion held as $Z^-H^+(PdO)$ is much less stable relative to $(PdO)_n$. Thus it appears that only a portion of the Pd in Pd–H-ZSM-5 can be highly dispersed and that portion depends on the presence of pairs of Brønsted acid sites in close proximity. The possibility of a link between the maximum in activity for NO reduction by CH_4 observed by Resasco and coworkers (3), and the concentration of Al pair sites in the zeolite is currently under investigation.

CONCLUSIONS

The state of Pd in Pd–H-ZSM-5 has been investigated using infrared spectroscopy and mass spectrometry. Prior to reduction on a low-loaded catalyst, a majority of the Pd is present as $Z^-H^+(PdO)H^+Z^-$. CO reduction results in the formation of small Pd clusters. O_2 treatment only partially redisperses the Pd; however, exposure to NO causes a complete redispersion of the Pd. The driving force for redispersion by NO is facilitated by the strong PdO–(NO) bond. Reoxidation of the catalyst in NO following a CO reduction yields a decrease in the Brønsted acid groups equivalent to approximately 2 H^+/Pd. This suggests that the Pd, when atomically dispersed, is stabilized by two adjacent Brønsted acid protons as $Z^-H^+(PdO)H^+Z^-$ species. Comparison of oxidized high- and low-loaded samples shows that the amount of Pd^{n+} ($n = 1$–3) present is nearly independent of weight loading. The majority of Pd on the high-loaded catalyst is present as $(PdO)_n$. NO TPR experiments on the high-loaded sample suggest that $(PdO)_n$ can be dispersed in the presence of NO as $Z^-H^+(PdO)NO$ species. However, upon removal of NO $Z^-H^+(PdO)$ species are not stable relative to $(PdO)_n$.

ACKNOWLEDGMENTS

This work was supported in part by a grant from the Gas Research Institute under Contract N. 5093-260-2492. Facilities were provided by the Director of the Office of Basic Energy Sciences, Chemical Sciences Division, of the U.S. Department of Energy under Contract DE-AC03-76SF00098.

REFERENCES

1. Nishizaka, Y., and Misono, M., *Chem. Lett.* 1295 (1993).
2. Nishizaka, Y., and Misono, M., *Chem. Lett.* 2237 (1994).
3. Loughran, C. J., and Resasco, D. E., *Appl. Catal. B: Environ.* **7**, 113 (1995).
4. Ali, A., Alvarez, W., Loughran, C. J., and Resasco, D. E., *Appl. Catal. B: Environ.*, in press.
5. Homeyer, S. T., and Sachtler, W. M. H., *Appl. Catal.* **54**, 189 (1989).
6. Che, M., Dutel, J. F., Gallezot, P., and Primet, M., *J. Phys. Chem.* **80**, 2371 (1976).
7. Descorme, C., Fakche, A., Garbowski, E., Lecuyer, C., and Primet, M., *in* "Proceedings of the Gas Research Conference, 1995," p. 505.
8. Joly, J. F., Zanier-Szyldowski, N., Colin, S., Raatz, F., Saussey, J., and Lavalley, J. C., *Catal. Today* **9**, 31 (1991).
9. Sheu, L. L., Knözinger, H., and Sachtler, W. M. H., *J. Molec. Catal.* **57**, 61 (1989).
10. Romotowski, T., Komorek, J., Paukshtis, Y. A., and Yurchenko, E. N., *Zeolites* **11**, 497 (1991).
11. Tarasov, A. L., Shvets, V. A., and Kazanskii, V. B., *Kinet. Catal.* **30**, 340 (1987).
12. Palazov, A., Chang, C. C., and Kokes, R. J., *J. Catal.* **36**, 338 (1975).
13. Anderson, S. L., Mizushima, T., and Udagawa, Y., *J. Phys. Chem.* **95**, 6603 (1991).
14. Hicks, R. F., Qi, H., Young, M. L., and Lee, R. G., *J. Catal.* **122**, 280 (1990).
15. Hicks, R. F., Qi, H., Young, M. L., and Lee, R. G., *J. Catal.* **122**, 295 (1990).
16. Vannice, M. A., and Wang, S-Y., *J. Phys. Chem.* **85**, 2543 (1981).
17. Naccache, C., Primet, M., and Mathieu, M. V., *Adv. Chem. Ser.* **121**, 266 (1973).
18. Jacobs, P. A., and von Ballmoos, R., *J. Phys. Chem.* **86**, 3050 (1982).
19. Bordiga, S., Platero, E. E., Arean, C. O., Lamberti, C., and Zecchina, A., *J. Catal.* **137**, 179 (1992).
20. Kustov, L. M., Kazansky, V. B., Beran, S., Kubelkova, L., and Jiru, P., *J. Phys. Chem.* **91**, 5247 (1987).
21. Quin, G., Zheng, L., Xie, Y., and Wu, C., *J. Catal.* **95**, 609 (1985).
22. Hoost, T. E., Laframboise, K. A., and Otto, K., *Catal. Lett.* **33**, 105 (1995).
23. Davydov, A. A., and Shepot'ko, M. L., *Zh. Prikl. Spektrosk.* **49**, 815 (1988).
24. El Hamdaoui, A., Bergeret, G., Massardier, J., Primet, M., and Renouprez, A., *J. Catal.* **148**, 47 (1994).
25. Weber, W. H., Baird, R. J., and Graham, G. W., *J. Raman Spectrosc.* **19**, 239 (1988).
26. Sheu, L. L., Knözinger, H., and Sachtler, W. M. H., *J. Am. Chem. Soc.* **111**, 8125 (1989).
27. Stakheev, A. Y., and Sachtler, W. M. H., *J. Chem. Soc., Faraday Trans.* **87**, 3703 (1991).
28. Wichterlová, B., Dedecek, J., and Vondrová, A., *J. Phys. Chem.* **99**, 1066 (1995).
29. Rice, M. J., Chakraborty, A. K., and Bell, A. T., unpublished results.